The influence of temperature on the dielectric permittivity and complex electrical resistivity of porous media saturated with DNAPLs: a laboratory study

Mohammad Ali Iravani, Jacques Deparis, Hossein Davarzani, Stefan Colombano, Roger Guérin, Alexis Maineult

The influence of temperature on the dielectric permittivity and complex electrical resistivity of porous media saturated with DNAPLs: a laboratory study

Mohammad Ali Iravani[1,2], Jacques Deparis[1], Hossein Davarzani[1], Stefan Colombano[1], Roger Guérin[2], Alexis Maineult[2,*]

1) BRGM, French Geological Survey, 45060 Orléans, France

2) Sorbonne Université, CNRS, EPHE, UMR 7619 METIS, 75005 Paris, France

Short title: Temperature effects on electrical signatures of DNAPL-saturated media

* Corresponding author. E-mail: alexis.maineult@sorbonne-universite.fr, Tel: +33 (0)1 44 27 43 36

Highlights:

- Effects of temperature on electrical resistivity and relative permittivity.
- Using SIP & TDR to monitor evolution of complex resistivity and relative permittivity.
- Influence of water and DNAPLs saturations on geophysical parameters.
- Cole-Cole parameters are affected by temperature increase.

Intended for publication in the Journal of Applied Geophysics

Abstract

While some recent studies have discussed various effects of temperature on the electric and electromagnetic properties of multiphase porous media, the effect of temperature changes in multiphase porous media polluted by dense non-aqueous phase liquids (DNAPLs) has rarely been documented. We attempted to characterize how relative permittivity and electrical resistivity vary with temperature in multiphase porous media. The measurements were carried out using two different column sizes. Glass beads with a 1 mm diameter were used to simulate porous media. Spectral induced polarization (SIP) and time domain reflectometry (TDR) were used to measure complex electrical resistivity and relative permittivity, respectively. We investigated the geophysical characteristics of two DNAPLs, coal tar (CT) and chlorinated solvent (CS), from 20 to 50°C; ultra-pure water was used as the reference fluid. Experimental data on the relative permittivity and complex resistivity of pure water obey empirical models, validating our experimental setup and protocol. Results demonstrated that the real parts of relative permittivity and electrical resistivity are functions of temperature in the medium with the presence or absence of a solid phase. While we did not study the imaginary part of relative permittivity, our observations in the DNAPL samples indicated that temperature increases decreased the imaginary parts of the complex electrical resistivity of DNAPLs tested, whether in the presence or absence of the solid phase. Temperature dependency of relative permittivity and complex resistivity were also studied in multiphase porous media, after drainage (80 % DNAPL and 20 % water) and after imbibition (8 % DNAPL and 92 % water). The effect of temperature increases on complex resistivity has a secondary effect on frequency domain and Cole-Cole parameters. It was found that the relationship between temperature and resistivity is linear; therefore, resistivity temperature coefficients were obtained for water and both DNAPLs with the presence and absence of solid phase.

Keywords: Spectral induced polarization, dense non-aqueous phase liquids, time domain reflectometry, temperature, complex resistivity, relative dielectric permittivity.

1 Introduction

Interpreting the geophysical parameters acquired during monitoring of subsurface soil strata is an important component of soil remediation programs. These parameters play a key role in validating the accuracy and efficiency of remediation methods in soils contaminated with organic and industrial chemicals commonly referred to as DNAPLs (Dense non-aqueous phase liquids). All over the world in the last decade, many sites polluted by industrial activities were abandoned. Study of the factors contributing to the pollution and of the remediation itself has significant environmental and health benefits. There is a consensus about the fact that geophysical techniques are among effective methods for long term monitoring of clean-up processes in soils (e.g., Cardarelli and Di Filippo, 2009; Hwang et al., 2008; Snieder et al., 2007; Sogade et al., 2006; Brewster and Annan, 1994). Among geophysical techniques that can be used to monitor physical properties on contaminated sites, electrical and electromagnetic methods are now proved to be reliable monitoring techniques that provide multiple geophysical parameters such as electrical resistivity and relative dielectric permittivity (e.g., Seyfried and Grant ,2007; Binley et al., 2005). Electro-geophysical methods have been used in many studies, such as estimation of the shallow subsurface conditions (e.g., Romig, 2000), environmental and engineering applications (e.g., Grimm and Olhoeft, 2004; Briggs et al., 2004), and detection of light non-aqueous phase liquids (LNAPL) (e.g., Atekwana et al., 2000). In these applications, the purpose of geophysical testing is to identify technical challenges and assist with implementing solutions during the clean-up process. So studying and monitoring two geophysical parameters, relative permittivity and complex resistivity, can be useful geophysical tools to achieve this.

The remediation method that we consider here is the thermally enhanced (using conduction heating) recovery of coal tar (CT) by means of the "pump and treat" technique to extract and remove CT from polluted soil. According to rheological principles, when temperature increases, viscosity decreases and the pumping rate consequently increases (Ajo-Franklin et al., 2006). Among all auxiliary treatment methods, the thermally enhanced technique is one of the most helpful techniques compared to biological methods (Nathanail et al., 2011; Colombano et al., 2010). Thermally enhanced treatment is the effective remediation technique on deep and shallow soil clean-up processes. Soil digging, excavation, transport and heating make this a costly yet affordable technique in many remediation projects. The results from our laboratory measurements were used to model the temperature dependence of complex resistivity and relative permittivity to interpret geophysical field measurements. While we know that the application of this work is in a similar range of temperature variations, two important points are worth mentioning in what follows. First, in the corresponding ongoing field survey, the maximum heating temperature was 50 °C; therefore, we chose 50 °C as the maximum temperature to have the closest simulation of the field work in the lab. Second, choosing a lower temperature limitation compared to feasible field studies can be recognized as a challenge, but if that high temperature limitation in the field will be less than this study, it may give other researchers the option to use these results according to their temperature limitations. Changes in water and DNAPL saturations might have much greater impact on permittivity and resistivity compared to temperature, but after pumping DNAPLs in the contaminated soils, we face change in resistivity and relative permittivity of the soil. These variations are due to temperature and saturation changes. Independent study on the impact of each of these two factors to determine how effective each factor is a must. Recently, the authors have investigated effects of saturation changes on these two parameters with more details in a separate study.

1.1 Influence of temperature on relative permittivity: a review

One of the important parameters for understanding the electric and electromagnetic characteristics of a fluid is the relative dielectric permittivity, or dielectric constant. Relative permittivity $\varepsilon = \varepsilon' + i\varepsilon''$ is a complex frequency dependent parameter , where $\varepsilon'(f)$ is the real part and $\varepsilon''(f)$ is the imaginary part, f is the frequency of the excitation current, and i is the pure imaginary unit ($i^2 = -1$). In this study, we only worked with relative permittivity, equal to $\varepsilon_r = \varepsilon / \varepsilon_0$, where ε_0 is vacuum permittivity and has a value of approximately 8.85×10−12 F/m. In the controlled experimental laboratory setups described below, in which time domain reflectometry (TDR) probes model 5TE were used (See below for description), the results only related to the real part of the relative permittivity.

Direct TDR measurements are sensitive to the effect of the temperature. For instance, Malmberg and Maryott (1956) established a relationship between the relative permittivity of water and temperature (in the range 0 to 100°C) as below, using experimental methods:

$$\varepsilon' = 87.740 - 0.40008T + 9.398(10^{-4})T^2 - 1.410(10^{-6})T^3 \quad (1)$$

where T is the temperature (°C). They stated that the proposed equation has a maximum error of 1 %. They also stated that the dielectric constant of water decreases with temperature, but for air, the temperature change does not have a significant effect on relative permittivity. Nath and Dubey (1980) and Nath (1995) have investigated that common error of dielectric constant measurements is ±5 %. They carried out their experiments on binary liquid mixtures like trichloroethene ($CHClCCl_2$) at 1.8 MHz with a dielectrometer (Dekameter DK_{03}). They used the equation that was proposed by Malmberg and Maryott (1956) to calculate relative permittivity and a relationship for electrical conductivity of soil water as a function of temperature:

$$\sigma_{dc}(T) = \sigma_{dc(25°C)}\exp[-\Delta(2.033 \times 10^{-2} + 1.266 \times 10^{-4}\Delta + 2.464 \times 10^{-6}\Delta^2] \quad (2)$$

in which $\Delta = 25 - T$ and σ_{dc} is the electrical conductivity of soil water. Chen and Or (2006) used TDR to obtain dielectric permittivity and found that even for frequencies lower than 100 MHz, TDR probes clearly showed effects of temperature (5-55°C) and electrical conductivity (due to Maxwell-Wagner (M-W) effect that is the charge at the interface of two materials due to difference of their charge relaxation times) on dielectric permittivity. They expressed that the effective range of the TDRs used is greater than 100 MHz and at low frequency (<100 MHz) this influence (M-W effect) is not noticeable compared to the higher frequencies. For each 1 °C increase in temperature, they reported a 0.3 % decrease in the relative permittivity of water. For TDR model 5TE, Rosenbaum et al. (2011) proposed an empirical correction function for the temperature effect between 5 and 40°C, tested on eight different liquids. They noticed underestimated values of relative permittivity for temperatures over the range 5 to 25°C (-2.7 for EC-5 and -3.9 for 5TE) and overestimated values for 25 to 40°C (+3.6 for both TDRs). They identified strong correlation between permittivity and electrical conductivity with increasing electrical conductivity with adding salt content.

The influence of temperature on relative permittivity has also been discussed for different fluids. Shah and Tahir (2011) investigated the dielectric properties of oils such as corn oil, cottonseed oil, and polychlorinated biphenyl (PCB) over a temperature range of 25 to 70°C. The effect of temperature on relative permittivity of a soil polluted by oil (petroleum) as a NAPL have also discussed by Iordache et al. (2010) on microwave at frequency 2450 MHz. They have presented that the relative permittivity of the oils increase with temperature increase over the range of 10 to 90 °C. There, the increase in dielectric permittivity was related to the humidity values that relative permittivity varied from almost 20 % to 70 % for humidity 5 % to 30 %, respectively. Persson and Berndtsson (2002) tried to find a relation between relative permittivity (measured by TDR), NAPL saturation and electrical conductivity. By further validating the results using a mixing model, they demonstrated that TDR measures relative

permittivity values very well. Finally, in a study about two kinds of chlorinated solvent (CS), Ajo-Franklin et al. (2006) performed experiments to study the effects of temperature, acoustic velocity and frequency on trichloroethylene (TCE) and tetrachloroethylene (PCE). They fitted experimental data of temperature with a simple linear equation. They stated that the dielectric permittivity of all solvents decreased due to increasing temperature.

In porous media, Keller and Frischknecht (1966) found that the relative permittivity of dry rock depends on temperature especially at audio- and subaudio-frequency (<10 kHz). They have stated the relative permittivity of dry rock increased as a function of temperature but they reported an inverse relationship between dielectric permittivity and frequency. The ratio of variation in frequency domain is greater in low temperature (100 °K) compared to high temperature (850 °K). Seyfried and Grant (2007) have characterized the real and imaginary parts of complex relative permittivity for 19 different soils from different areas of the USA at frequency 50 MHz. They found 2 % $°C^{-1}$ change in the imaginary part of the dielectric constant similar to what was proposed by Campbell et al. (1949) for soil's electrical conductivity. This effect is six times less for the real part of the relative permittivity as a function of temperature.

1.2 Effect of temperature on complex resistivity: a review

According to Ohm's law, electrical resistivity is the ratio of the electrical current over the applied electric field. The applied electric field is closely related to the current behavior (e.g., Wightman et al., 2004). Electrical resistivity is a complex value described by $\rho = \rho' + i\rho''$ in which $\rho'(f)$ and $\rho''(f)$ are the real and imaginary parts of the complex resistivity, respectively $i^2 = -1$. Note that electrical resistivity (ρ) is the inverse of electrical conductivity σ ($\sigma = \rho^{-1}$).

Many studies have found that temperature has a strong effect on the electrical resistivity of subsurface strata (e.g., Sen and Goode, 1992; Waxman and Thomas, 1974). Electrical resistivity decreases as temperature increases in water (Chen and Or, 2006; Hayashi, 2004; Weast, 1986; Stogryn, 1971), vegetable oil (Lakrari et al., 2013), semiconductors (Keller and

148 Frischknecht, 1966), ionic fluids (Noritomi, 1958), permeable water-saturated rocks (Binley et
149 al., 2010; Llera et al., 1990; Coster, 1948), sodium chloride solutions (Arps, 1953), different
150 soil types (Nouveau et al., 2016) and soil zones (Sherrod et al., 2012).

151 To find a relationship between temperature and conductivity (or resistivity), Campbell
152 et al. (1949) provided the effect of temperature change on electrical conductivity of 30 different
153 saturated soil samples from different regions of the USA and India. They found that electrical
154 conductivity changed by approximately 2.02 % and 1.79 % per degree of temperature change
155 over the range of 15 to 35°C and 0 to 15°C, respectively. Before this research, for many years,
156 a table issued by Whitney and Briggs (1897) was a guide for researchers to adjust soil resistance
157 at a given temperature; Richards (1954) published another table to correct temperature for
158 multiple soil samples. The results of Chen and Or (2006) supported further those by Campbell
159 et al. (1949), i.e. an approximately 2 % increase in electrical conductivity for each degree
160 centigrade change in temperature. They also reported that increasing concentration of
161 suspended material decreases how electrical conductivity depends on temperature. Hayashi
162 (2004) evaluated electrical conductivity during mixing of water and saline water with different
163 compositions and its dependency on temperature. They tested the arbitrary constant of a 2 %
164 increase in electrical conductivity per 1°C, which was proposed by Campbell et al. (1949). They
165 discovered that the relationship is non-linear when temperature is between 0 and 30°C but a
166 linear relationship could also estimate the variation reasonably. Above 30°C, it appeared that a
167 viscosity-based relation estimated the electrical conductivity better than the temperature-based
168 relation. Hayley et al. (2007) modified a petrophysical model over a temperature range of 0-
169 25°C. Between the exponential Arrhenius equation and the linear equation proposed by
170 Campbell et al. (1949), linear approximation has properly predicted the results at low
171 temperatures. Arps (1953) has discussed the relationship between electrical resistivity,
172 temperature, and sodium chloride concentration (SCC). Sen and Goode (1992) have published

an equation showing the relationship between temperature and electrical conductivity. They compared the results of their model with Arps (1953) formula and found that their relation could better predict the conductivity variations. Finally, Grellier et al. (2006) investigated the effect of temperature on the electrical conductivity of leachate. They showed the electrical conductivity of leachate alone and granular media saturated with leachate as a function of temperature. They separately demonstrated their results for pure leachate and a granular sample saturated with leachate.

Many materials and compounds are semiconductors, including those based on the periodic table's carbon group, like silicon, and binary compounds between different group elements like silicon carbide and organic semiconductors, oxides and alloys. For semiconductors, Keller and Frischknecht (1966) have stated that temperature increase has a direct impact on the amplitude of ion movement and vibration. It also has an exponential effect on how frequently ions jump into the vacancies after temperature increases. All semiconductors have negative temperature coefficients of resistivity. Noritomi (1958) published the curve of an ionic fluid for conductivity as a function of temperature. It showed the inverse relation between conductivity and temperature.

Keller and Frischknecht (1966) have also published the effect of temperature on the resistivity of water-bearing rocks. They found that at normal temperatures (moderate temperature around 18 to 25 °C), electrical resistivity (conductivity) is related to the resistivity (conductivity) of the electrolyte in rocks. Moreover, they found that the resistivity of water decreased as its viscosity decreased (because of temperature increase). They identified that for the same rock, resistivity at 12 °C is 10 to 100 times higher than resistivity at 18 °C. Focusing on water-bearing rocks, Binley et al. (2010) worked on the effects of temperature on the real and imaginary parts of electrical conductivity and the spectra of three permeable sandstones (Berea, Cottaer and Sherwood with porosity of 19, 21 and 32 % , respectively) at 1.5 Hz. For

198 simplicity, they developed a simple model to study the relaxation time related to the peak of the
199 imaginary part of electrical conductivity rather than theoretical and phenomenological models
200 like Cole-Cole model, successfully for the experimental data. Llera et al. (1990) proposed a
201 quasi-exponential relation between temperature and resistivity of water-saturated rocks. This
202 relation also confirmed the decrease in resistivity with temperature increases above 200°C
203 induced by high pressure. Coster (1948) found that at high temperature (up to 1000 °C),
204 conductivity of rocks increased exponentially with temperature for seven rocks tested. They
205 used DC current to measure the resistance and then calculate conductivity. They published a
206 table demonstrating the dependency of conductivity, temperature, and depth. Not only for
207 different soil types (Nouveau et al., 2016), but also Sherrod et al. (2012) have provided the data
208 for apparent resistivity and temperature monitoring for 3 years in different soil zones in a
209 moderately heterogeneous shallow field subsurface. They have published equations for the
210 relationship between temperature and resistivity in the vadose zone (to the depth of almost 1 m)
211 and saturated zone (at depth among 1 to2 m). Due to seasonal variations in precipitation during
212 the measurement period, they clearly monitored the effects of drainage and imbibition in the
213 shallow subsurface. Finally, Zhu et al. (2018) have described the electrical properties of five
214 coal samples. At low and high temperatures (30 to 200 °C), they prepared two complex
215 resistivity-temperature and complex relative permittivity-temperature models by separately
216 measuring electrical impedance in samples. Subsequently, complex resistivity and relative
217 permittivity were obtained by calculation. They found that at low frequencies (less than
218 100 kHz), volume resistivity rapidly decreased, but the rate of decrease at medium (100 kHz to
219 10 MHz) to high frequencies (10 to 30 MHz) was much slower. At a fixed frequency (100 kHz),
220 with temperature increase, volume resistivity initially increased, but it conversely decreased at
221 the end. They reported that both the real and imaginary parts of relative permittivity had the
222 inverse behavior than temperature increases.

Some studies reported inverse behavior for how resistivity changed with temperature. For instance, Quist and Marshall (1968) found that for water in some specific conditions, dielectric permittivity decreased but electrical resistivity increased for temperatures above 300°C. In a study on lateritic soil, Bai et al. (2013) found that the electrical resistivity decreased non-linearly with increasing temperature.

1.3 Objectives

Studies on DNAPLs, which are non-polar insulators, are harder than studies on polar water due to heterogeneity in DNAPLs resulting from weathering and biodegradation (Ajo-Franklin et al., 2006). It is interesting from the geophysical standpoint to study how these two fluids with different polarity and dielectric properties interact after drainage and after imbibition of water on soil and comparing the results with results obtained from pure products. Some studies have reported effects of soil heating on different liquids and materials like NAPLs but little attention has been paid to effects of temperature change on soils polluted by DNAPLs and their electro-geophysical characteristics. A lack of study and data regarding how to clean up pollution in these contaminated soils and porous media from the geophysical perspective in the literature. After years of geophysical study, debate continues to swirl around this subject.

The aim of this experimental study was to assess the effects of temperature changes on the complex electrical resistivity, relative permittivity, and temperature coefficient for the conductivity, for two different types of DNAPLs (i.e., CT and CS) and water in porous media. This study examined the application of spectral induced polarization (SIP) and TDR as electro-geophysical methods for estimating the efficiency of soil heating methods used as remediation processes for sites polluted by DNAPLs.

This research provides a better understanding of how effective thermal enhancement is, highlights the dependency of geophysical parameters on temperature change for DNAPL remediation, and could be useful for accelerating the remediation process by choosing the

optimum temperature in soil heating techniques. Choosing the optimal temperature can be a critical issue. Firstly, this temperature should be less than heat of vaporization of the DNAPLs because smelling DNAPL vapor can be very hazardous. Secondly, as far as increasing temperature caused decreases and increases in electrical resistivity and dielectric permittivity (measured by TDR) respectively, the higher temperature heating leads to the faster DNAPL recovery. In the following part, we express the experimental setups to obtain these goals.

2 Experimental setups and data acquisition

The methodology used in this study is based on the laboratory experiments carried out to estimate electrical resistivity and relative permittivity of multiphase porous media developed recently by Colombano et al. (2017). The complex resistivity data were collected using SIP. Resistivity measurements were taken at 20 frequencies ranging from 0.183 Hz to 20 kHz. Relative permittivity values were obtained from 5TE TDR probes (METER Group), at 70 MHz (to diminish salinity and textural effects to obtain data that are more comprehensive (Kizito et al., 2008)).

Laboratory tests were carried out on cells and columns. All cells and columns were made of polyvinylidene fluoride (PVDF), a highly non-reactive, thermoplastic polymer normally used when strong solvent-resistance is needed (Schweitzer, 2004). Coarse glass beads (GB) with a diameter of 1 mm were used to simulate a porous medium. Water saturations, DNAPL saturations, and temperature variation were used as the variables in the experimental program. CT and CS with water were used to model a two-phase fluid system. In our experiments, water was treated as the reference liquid to compare the results of contaminations and to monitor the effects of pollution removal in porous media. Table 1 shows both DNAPL's (CT and CS) properties at 20°C. In all experimental setups, one measurement and six measurements were done in the small cell and the columns, respectively (Fig. 1.).

Fig. 1 shows a schematic layout of the cell and the column used in this study. Each experimental setup has three main parts: water reservoir, DNAPL reservoir and main column (porous medium). The cells were 5.56 cm long with the internal diameter of 5.8 cm, but the columns were 25 cm long with the same internal diameter. Each of the main samples was connected to a DNAPL reservoir and a water reservoir with plastic tubes with internal diameters of 3.5 cm, and 36 cm and 8 cm long, respectively.

The distribution of the electrical potential in porous media around two current-carrying electrodes depends on the electrical resistivity and distribution of the surrounding media. In the laboratory measurements with the configurations of Wenner alpha and Schlumberger for cells and columns, respectively, an AC current was applied between two ring-current electrodes implanted in the columns and two potential electrodes used to collect the potential difference. In these configurations, all the electrodes were embedded on the same orientation and the electrodes for measuring M and N were laid out between the current electrodes A and B. As illustrated in Fig. 1., according to the principles of these configurations, for Wenner alpha distances between two electrodes next to each other are same, but for Schlumberger the distance MN is small compared to AB.

For the small cells and columns, two and six non-polarizable hand-made $Cu/CuSO_4$ potential electrodes (Maineult et al., 2004) were installed between the two current electrodes, respectively. The two metallic ring current electrodes that are made of nickel-cobalt alloy (MP35N) were placed on the top and bottom of cells and columns. These current electrodes had the same diameters as the internal diameter of the columns. For the potential electrodes, the saturating solution was made of milli-Q water (ultrapure water) 72.75 %, $CuSO_4$ 26 % and gelatin 1.25 % that were mixed and heated (≈80°C) for 45 minutes using a shaking heating plate. The stability and reliability of these potential electrodes was checked by performing resistivity measurements of tap water 12 hours before running and ending experiments. These

297 measurements with the water also helped us to find the geometric factors of each sample for
298 calculating the resistivity values from measured impedance. The conductivity and temperature
299 of water also measured with a portable conductivity meter, model pH/Cond 340i (WTW
300 Measurement System Inc.) before starting experiments to obtain thegeometric factor of each
301 sample. Finally, the SIP measurements were done using the SIP-lab-IV instrument (Radic
302 Research).

303 Relative permittivities of each cell and column were measured with 10 cm (l) ×3.2 cm
304 (w) model 5TE TDR sensors and cable length of 5 m located at the middle of the cells and
305 columns (Fig. 1.). The effective zones of the TDRs were examined in a complex multiphase
306 sample before designing the cells and columns; the radius of influence of these TDRs is 2.5 cm
307 in all directions. There were one TDR in cells and three TDRs in columns. All TDRs were
308 connected to a CR-1000 data logger (Campbell Scientific Inc.), in order to independently
309 monitor the relative permittivity and temperature in our porous medium.

310 The temperature variations were applied first on pure products with and without GB,
311 second in glass beads packed after drainage and third after imbibition. During the first stage
312 (experiments on pure products), the geophysical characteristics of water, CT and CS were
313 obtained to facilitate comparing and understanding the effects of saturation of each phase
314 besides temperature in the next stages.

315 The second and the third experimental setups, i.e., after drainage (wetting phase
316 irreducible saturation) and after imbibition (non-wetting phase residual saturation), were
317 designed to obtain measurements in different contaminant saturations over time and frequency.
318 In our experimental setups, the DNAPL saturation after drainage was 80 % ± 1 % and water
319 saturation was 20 % ± 1 %. The ratios of water and pollution were 92 % and 8 % ± 1 %,
320 respectively. With these experimental setups, we planned to evaluate the effect of temperature

change in different saturations to estimate correctly the DNAPL saturations during the remediation processes.

Before starting drainage, degassed-tap water obtained from an ultrasound tank (VWR Ultrasonic Cleaner - USC500D) was injected into the cells/columns from the valve placed at the bottom by a peristaltic pump (Watson Marlow 530U). Drainage and imbibition were simulated by increasing and decreasing level of the DNAPL column at the left side of the cell and water reservoir. The methodological approach taken in this study is based on the variation of electrical resistivity and relative permittivity due to temperature increase throughout the different experimental setups. In all setups, experiments were launched at 20°C then the temperature was increased to 30°C, 40°C, and 50°C after 24 hours or in some cases after a shorter period of time but never less than 12 hours. The oven used for this study was isolated and had a temperature sensor inside it. All measurements were recorded as soon as the same temperatures were obtained inside the samples (recorded by TDRs) and the oven. In our experiments, all these geophysical parameters were measured in a regular time schedule of two hours for complex resistivity and thirty seconds for relative permittivity.

3 Results

3.1 Effects of temperature on the relative permittivity

TDRs separately collected relative permittivity data during simultaneous experiments on cells and columns. As we mentioned in section 2, all the TDR probes were placed inside the columns. When the temperature was increased, one hour of delay was observed in the reported temperature from TDRs. Because 70 MHz was the applying frequency of the TDRs used in this study, the real part of the complex permittivity was much more than the imaginary part (e.g., for water it is≈81 versus ≈2) (Raju, 2003), therefore, only the real part of the complex frequency

dependent absolute permittivity of water and DNAPLs were considered to obtain the relative (dielectric) permittivity.

3.1.1 Effects of temperature on the relative permittivity of pure products

The first sets of analyses examined the impact of temperature increases on the pure products. The results of the analysis of relative permittivity data for pure product with and without GB for different temperatures are presented in Fig. 2. It is apparent that temperature increase decreases the relative permittivity of water with and without GB. On the contrary, in the columns saturated with CT or CS, temperature increases increased relative permittivity. This could be because both DNAPLs are non-ionic fluids whereas water is an ionic fluid (Riley, 1988). The relative permittivity of the columns saturated with CT, with and without GB, was higher than the relative permittivity of columns saturated with CS. These results also evidence the effect of adding GB to the medium. In three columns with GB, adding GB led to a 2.37 to 2.15 times decrease in the relative permittivity of water over the range of 20 to 50°C, but in the DNAPL columns, it increased the relative permittivity of almost 1.7 to 1.77 and of 1.85 to 1.77, respectively. This inverse behavior of CT and CS compared to water is because the relative permittivity of GB is higher than the relative permittivity of CT and CS, but lower than the relative permittivity of water.

From the data concerning water, we can see that the temperature change from 20 to 30°C had a lower slope than the next temperature increase. Temperature increases led to 29.04 %, 19.91 %, 23.59 % and 24.80 % increases in the relative permittivity of CS, CT, GB+CS and GB+CT over the range of 20 to 50°C.

3.1.2 Effects of temperature on relative permittivity after drainage (irreducible wetting phase saturation) and imbibition (residual non-wetting phase saturation)

DNAPLs as a non-wetting fluid and water as a wetting fluid were used as two different liquid phases. Experiments on the columns were performed with gradual draining of main

samples by increasing the DNAPL reservoir column with incremental steps. After replacing the non-wetting phase by the wetting phase, the experiments were stopped and the temperature increased, as we did for pure products. How relative permittivity (real part) changed for both DNAPLs after drainage and imbibition over the temperature range of 20 to 50°C is presented in Fig. 3. The DNAPLs and water saturations were about 80 % and 20 % after the drainage stage, respectively, but these proportions were respectively 8 % and 92 % after imbibition. Analyzing these two stages needs the reference data of pure DNAPLs and water with GB (100 % DNAPLs and 100 % water) that are also presented in Fig. 3.

From this data, after drainage, because of DNAPL saturation dominating compared to water, it was apparent that the relative permittivity of both DNAPLs increased with increasing temperature. During the experiments, sometimes a slight difference between the permittivity of the different columns with the same DNAPL was observed. It could be because of the difference in geometry and the amount and distribution of DNAPL saturations of cell and column. Heterogeneity in the distribution of pollutants may explain these discrepancies between the different columns saturated with the same pollutant. After drainage, for both CS+GB and CT+GB, the trends of the results agreed with the results for pure products (see Fig. 2).

After rewetting the sample by replacing water with DNAPLs (by decreasing the DNAPL reservoir column), the residual DNAPL saturation could not be removed from the sample. In this stage, the measured relative permittivity was used, in order to assess the temperature increase after imbibition with the residual non-wetting saturations. Because water saturation (92 %) was much higher than DNAPL saturation (8 %), temperature increases should normally cause a permittivity decrease. As shown in Fig. 3, the variation of relative permittivity as a function of temperature after imbibition for CS follows the water trend precisely but for the CT column, this variation was constant with a slight increase. It seems possible that these results were due to DNAPL saturation of more than 8 % after imbibition in this column. It is helpful to note that

after finishing the experiment and while the columns were being cleaned, it was obvious that CT saturation was higher than CS saturation in these columns. It seems that the higher adhesion of CT compared to CS tends make it stick to the glass beads and increase the residual saturation.

3.2 Effects of temperature on the electrical resistivity

The electrical resistivity of a porous medium contaminated by DNAPLs depends on many geological, geophysical and environmental factors but the most important parameters are proportionality of water and DNAPL saturations, porosity of the porous media, salinity and temperature. The dominant conductor between water and DNAPL and the degree of saturation of each fluid in the porous media have important effects on electrical complex resistivity. In the following sections, we focus on the effects of how varying water and DNAPL saturations and temperature change affect the real and imaginary parts of the complex electrical resistivity.

3.2.1 Effects of temperature on the electrical resistivity of pure products

To have a better understanding of how temperature changes regulate and affect resistivity values, Fig. 4 summarizes all measurements to show how resistivity (real part) and phase spectra (imaginary part) of complex resistivity of pure products change as a function of temperature at 1.46 Hz. Temperature increases decreased resistivity values for water and two DNAPLs with and without GB. Adding GB to the samples increased resistivity for water and decreased resistivity for both DNAPLs.

Resistivity was higher for CS than for CT. This difference is more significant at 20°C and from 30 to 50°C the resistivity values were close to each other. Higher decreases in resistivity for columns of CT and CS were observed from 20 to 30°C compared to the other temperature changes. From this data, resistivity of water and GB+water also decreased with temperature increases, with the same slope.

Phase shift spectra in water samples with and without GB were constant between 0 to 2 mrad but temperature increases decreased phase spectra for both pollutants with and without

GB. Compared to the amplitude of complex resistivity, phase shift was not significantly affected by adding GB for CT but for CS, a significant change in phase was observed, especially at 40 and 50 °C. Generally, in all samples with DNAPLs, temperature increases decreased both the real and imaginary parts of complex resistivity (electrical resistivity and phase).

3.2.2 Effects of temperature on the electrical resistivity after drainage (irreducible wetting phase saturation) and after imbibition (residual non-wetting phase saturation)

As investigated in section 3.2.1, after performing measurements on pure products, all the experiments were done after drainage and after imbibition, respectively, to see the effects of temperature for different phase saturations in a multiphase system. Fig. 5 shows how resistivity and phase carried as a function of temperature for all columns, after drainage, after imbibition and for pure products. After drainage and imbibition, resistivity linearly decreased due to temperature increases for both DNAPLs. The influence of 20 % water after drainage compare to the pure products is clearly evidenced in Fig. 5. As we expected, resistivity was higher in pure products than after drainage but the downward trends were almost the same.

The difference between the resistivity of both DNAPLs after imbibition with water were very low. After imbibition, the domination of water saturation versus DNAPLs saturation in these columns could be the reason for this similarity and low differences (because of regular behavior of water compared to DNAPLs).

For CS, temperature increases decreased the phase spectra after drainage and after imbibition like pure products but for CT, after drainage and after imbibition the phase spectra decreased and increased as a function of temperature, respectively.

3.3 Frequency domain of electrical resistivity and phase

Amplitude and phase spectra obtained from SIP response of the samples of CT with and without GB at all frequencies are shown in Fig. 6. The results of laboratory spectra show that

temperature increases decreased resistivity for both cases. The difference in resistivity was more significant in low frequencies than for high frequencies.

Phase spectra of both CT and GB+CT show that increasing temperature shifts the bell curve (peak) to the higher frequency. This finding is consistent with those of Binley et al. (2010) about the effect of temperature change on phase spectra at the frequency range of 0.002 to 100 Hz. As they explained, this expected phenomenon is because of lower relaxation time for the diffusive process. The experiments on the other DNAPL (CS) with and without GB followed the same trend for both the real and imaginary parts of complex resistivity but the peak of the bell shape curve was at a lower frequency that for CT.

4 Discussion

4.1 Empirical models for relative permittivity

Our experimental data for the relative permittivity of pure water (Fig. 7) corroborated previous research (Lide, 2008; Weast, 1986; Malmberg and Maryott, 1956 (see Equation 1)). Weast (1986) proposed an equation to study the real part of relative permittivity of pure water as a function of temperature:

$$\varepsilon' = 78.54[1 - 4.58 \times 10^{-3}(T - 25) + 1.19 \times 10^{-5}(T - 25)^2 - 2.8 \times 10^{-8}(T - 25)^3] \quad (3),$$

whereas Lide (2008) gave the following relation:

$$\varepsilon' = 0.24921 \times 10^3 - 0.79069T + 0.72997 \times 10^{-3}T^2 \quad (4),$$

where in this equation T is the absolute temperature in °K. In Fig. 7, there is a similarity between the trend of measured relative permittivity of water in this study and past studies. Our experimental data fell within the area between the curves obtained by Malmberg and Maryott (1956), Weast (1986) and Lide (2008). In Fig. 7, the curves of Lide (2008) and Malmberg and Maryott (1956) are completely superimposed. The fact that our results are in agreement with

468 the expected behavior of pure water makes us confident of the validity of the measurements for
469 other compounds and multiphase media.

470 Two different experimental setups, a cell with one TDR and a column with three TDRs,
471 recorded values every thirty seconds after increasing temperature for each step, therefore,
472 hundreds of data points were obtained for each TDR for a given temperature. Since changes in
473 recorded relative permittivity were very low, mean values with standard deviation less than
474 0.05 (for all compounds) were used to show the permittivity for each temperature in Fig. 2. For
475 other compounds, we fit the permittivity change with temperature using the following equation:

476 $$\varepsilon' = \varepsilon'_{20} + a(T-20) + b(T-20)^2 \quad (5)$$

477 where T is temperature in °C. After fitting the experimental data, the obtained coefficients ε'_{20},
478 a and b, adjustment coefficient (R^2) and *p-value* are reported for our different multiphase
479 systems in Table 2. In terms of statistical changes, our calculated R^2 and *p-value* for all three
480 compounds were significantly fitted; therefore, the proposed models have reasonable
481 predictions of experimental data.

482 One of the empirical mixing models for relative permittivity in multiphase porous media
483 at high frequency (more than 100 GHz) is the CRIM (Complete Refractive Index Method)
484 model (Glover, 2015), which for our experimental setups can be expressed as:

485 $$\varepsilon_{mixed} = (\varphi\sqrt{\varepsilon_{water,CT\ or\ CS}} + (1-\varphi)\sqrt{\varepsilon_{GB}})^2 \quad (6)$$

486 where ε is the relative permittivity and φ is the porosity of the medium. CRIM model is a
487 derivative (when $m = 2$) of a general empirical mixing model for relative permittivity that is
488 called the Lichtenecker–Rother equation (Glover, 2015):

489 $$\varepsilon_{mixed} = (\sum_{i=1}^{n} \varepsilon_i^{1/m} \varphi^i)^m \quad (7)$$

490 In this equation m is a frequency-dependent coefficient that can vary for different frequencies
491 in both high and low frequency but in high frequency, the polarization factor will affect the

relative permittivity of water (Glover, 2015). From our experimental data, the porosity is 38 ± 2 %, and we assume that the relative permittivity of glass beads is 13.8. In Fig. 8, the CRIM model properly fit the experimental data for water and CT at 20 and 30°C but there are small underestimations at 40 and 50°C. For CS, the CRIM model has an underestimation over the temperature range of 20 to 50°C but the trend of predicted relative permittivity matches the experimental data for this DNAPL. As equation 6 shows, the CRIM model is a relationship between a material's permittivity and its volume fractions in a multiphase system. Correction of this equation by adding temperature effects can avoid inaccurate data estimations for high temperatures.

For CS, temperature increases led to a greater difference between experimental and predicted data.

4.2 Temperature coefficient of resistivity (α)

How the electrical resistivity of water and other materials varies has been widely studied. For instance, the resistivity of metals and semiconductors respectively increase and decrease with temperature increase, but alloys' resistivities do not have very strong temperature dependency (Keller and Frischknecht, 1966).

Dakhnov (1962) and Keller and Frischknecht (1966) have presented a relation to describe the temperature dependency of resistivity for an aqueous liquid over the temperature range of 0-200°C:

$$\rho_w = \frac{\rho_{w_0}}{1+\alpha(T-T_0)} \quad (8)$$

where ρ_{w0} is the resistivity of the aqueous fluid at temperature T_0 and α is the temperature coefficient of resistivity. From our result, the calculated α for water is 0.027°C^{-1}. This finding is in agreement with Keller and Frischknecht (1966) and Campbell et al. (1949), who showed that α is about 0.025 and 0.02°C^{-1}, respectively. Hayley et al. (2007) and Scott and Kay (1988)

have reported a range of temperature coefficient between 0.018 - 0.022 for water. Heimovaara et al. (1995) and Amente et al. (2000) also published 0.019 for water. For unsaturated soil in a field scale, Nouveau et al. (2016) found α value of 3-3.5 %. They stated that the main reason for this difference with the past work could be because of using resistivity data after inversion.

This equation for an ionic salty aqueous solution showed that resistivity and temperature have are inversely connected. For water, increasing mobility of ions because of temperature increase decreased viscosity. One of the main challenges in this study was verifying this relation for two different DNAPLs as non-ionic fluids. According to an intuitive hypothesis, after monitoring the trend in resistivity variation with temperature in our experimental data and accuracy and precision of fitting, temperature coefficients for resistivity were obtained for all measurements in all cells and columns. In some cases, the parabolic equation had the better fitting with adjustment coefficient (R^2) almost equal to one, but with the parabolic fitting the final equation is more complicated. The results of linear fitting of DNAPL data properly demonstrated the accuracy of the equation proposed by Dakhnov (1962) for both DNAPLs.

Fig. 9 shows the linear method that was used to obtain the α coefficient and α value for all cells and columns. The CS α value is much higher than the α values for CT and water, but we saw less variation in α values when they are with GB. By contrast with both DNAPLs, adding GB increased the α value of water from 2.7 % to 5 %.

4.3 Effect of temperature on Cole-Cole parameters

Pelton et al. (1978) discussed the relevance of induced polarization and the Cole-Cole model. The Cole-Cole presents the resistivity of a porous medium as:

$$\rho(\omega) = \rho_0 \left[1 - m(1 - \frac{1}{1+(i\omega\tau)^c}\right] \quad (9)$$

How the four major parameters in the Cole-Cole model (with the code developed by Maineult et al., 2017), low frequency resistivity ρ_0,intrinsic chargeability m, Cole Cole exponent c and

mean relaxation time τ that characterizes the decay (Pelton and Smith, 1976) change as a function of temperature for CT, with and without GB, is shown in Fig. 10. Increasing temperature increases ρ_0, m, log(τ) but parameter c fell after a change from 40 to 50°C for CT. Temperature increases decreased ρ and log(τ) and increased m but after 40°C this parameter became constant. c was also constant and equal to 1, that is conform with the Debye model (Kalmykov et al., 2004).

5 Conclusions

This study attempted to extend our understanding of how temperature changes affect relative permittivity and complex electrical resistivity in multiphase porous media saturated with coal tar or chlorinated solvent. Our findings enhance knowledge on auxiliary techniques (e.g., thermally enhanced DNAPL remediation techniques), which accelerates clean-up processes (pump and treat) for sites polluted by DNAPLs. Whether a solid phase was present or absent in the experiment, results showed that as temperature increased, the real component of the relative permittivity of water and DNAPLs decreased and increased, respectively. Adding solid phase to pure samples increased and decreased the relative permittivity of DNAPLs and water, respectively. The effect of temperature change on relative permittivity of both DNAPLs was the same as for pure DNAPLs but after imbibition (8 % DNAPL and 92 % water), unlike CT, the relative permittivity of CS samples did not conform to the relative permittivity of pure CS.

Temperature increased decreased both the amplitude and phase shift component of the electrical resistivity of water and both DNAPLs tested in the presence or absence of the solid phase. How Cole-Cole parameters change as a function of temperature were also discussed in this study. The laboratory spectra showed temperature increases decreased resistivity on the frequency domain for CT in the presence or absence of the solid phase. It was found that the

564 difference in resistivity was more significant for low frequencies than for higher frequencies.
565 Laboratory phase spectra of both CT and GB+CT showed that increasing temperature shifted
566 the bell curve of the spectrum to higher frequency. Our experimental data of electrical complex
567 resistivity and relative permittivity conform to the empirical models on these subjects.

568 These current results demonstrated that SIP and TDRs follow variations in electrical
569 resistivity and relative permittivity during the long-term monitoring of soil remediation
570 processes. The GB diameter was purposefully selected to simulate the same physical
571 characteristics in laboratory setups and our targeted fieldwork (e.g., same porosity in the lab
572 (38 % ± 2 %) and the field (36 % to 42 %)). Results compared with empirical models and can
573 be extended to field work. In general, we believe that these results might be applied to sandy
574 soils and permeable sandstones with close porosity and resistivity but we cannot claim that
575 these findings would be suited to other soils with different porosities and resistivity because the
576 electrical resistivity of soils is related to their composition and corresponding physical indexes
577 like the plasticity index, coarse function and more (Abu-Hassanein et al., 1996).

578 In the field, the body of porous media are soils with lower resistivity and higher relative
579 permittivity compared to GB. We believe that along with its benefits, using GB may influence
580 the temperature dependency of a medium but this difference should not be significant unless
581 particularly fine-grained soil with high electrical conductivity will be used.

582 Finally, we found that changes due to temperature are not really significant on relative
583 permittivity but that combining resistivity and TDR data could be a key point. Further research
584 on the effects of temperature change on the imaginary component of relative permittivity is
585 needed. Additional research on geophysical characteristics of other DNAPLs will expand the
586 application of this study.

587 **Acknowledgements**

588 This study was performed as part of the BIOXYVAL project. The authors would like to thank
589 ADEME for funding part of the project under the “Investissements d'Avenir” program, BRGM,
590 Iranian consulting engineers “Hegmatan-Mahar Ab” for providing the PhD thesis scholarship
591 of Mohammad Ali Iravani, and Nicolas Philippe, Benjamin Douche from BRGM and Setareh
592 Behjatamin for valuable experimental assistance. Finally, we gratefully acknowledge the
593 financial support provided to the PIVOTS project by the “Région Centre – Val de Loire” and
594 the European Regional Development Fund.

595 6 References

596 Abu-Hassanein, Z.S., Benson, C.H. and Blotz, L.R., 1996. Electrical resistivity of compacted
597 clays. Journal of geotechnical engineering, 122(5), 397-406.

598 Ajo-Franklin, J. B., Geller, J. T. and Harris, J. M., 2006. A survey of the geophysical properties
599 of chlorinated dnapls. Journal of Applied Geophysics 59(3), 177–189.

600 Amente, G., Baker, J. M. and Reece, C. F., 2000. Estimation of soil solution electrical
601 conductivity from bulk soil electrical conductivity in sandy soils. Soil Science Society of
602 America Journal 64(6), 1931–1939.

603 Arps, J., 1953. The effect of temperature on the density and electrical resistivity of sodium
604 chloride solutions. Journal of Petroleum Technology 5(10), 17–20.

605 Atekwana, E. A., Sauck, W. A. and Werkema Jr, D. D., 2000. Investigations of geoelectrical
606 signatures at a hydrocarbon contaminated site. Journal of Applied Geophysics 44(2-3), 167–
607 180.

608 Bai, W., Kong, L. and Guo, A., 2013. Effects of physical properties on electrical conductivity
609 of compacted lateritic soil. Journal of Rock Mechanics and Geotechnical Engineering
610 5(5), 406–411.

611 Binley, A., Slater, L.D., Fukes, M. and Cassiani, G., 2005. Relationship between spectral
612 induced polarization and hydraulic properties of saturated and unsaturated sandstone. Water
613 resources research, 41(12), W12417.

614 Binley, A., Kruschwitz, S., Lesmes, D. and Kettridge, N., 2010. Exploiting the temperature
615 effects on low frequency electrical spectra of sandstone: A comparison of effective diffusion
616 path lengths. Geophysics 75(6), A43–A46.

617 Brewster, M. L. and Annan, A. P., 1994. Ground-penetrating radar monitoring of a controlled
618 DNAPL release: 200 MHz radar. Geophysics 59(8), 1211–1221.

619 Briggs, V., Sogade, J., Minsley, B. J., Lambert, M., Reppert, P., Coles, D., Rossabi, J., Riha,
620 B., Shi, W. and Morgan, F. D., 2004. Mapping of TCE and PCE contaminant plumes using a
621 3-D induced polarization borehole data. Symposium on the Application of Geophysics to
622 Engineering and Environmental Problems, Environmental and Engineering Geophysical
623 Society, pp. 472–483.

624 Campbell, R., Bower, C. and Richards, L., 1949. Change of electrical conductivity with
625 temperature and the relation of osmotic pressure to electrical conductivity and ion concentration
626 for soil extracts. Soil Science Society of America Journal 13(C), 66–69.

627 Cardarelli, E. and Di Filippo, G., 2009. Electrical resistivity and induced polarization
628 tomography in identifying the plume of chlorinated hydrocarbons in sedimentary formation: a
629 case study in rho (Milan-Italy). Waste Management & Research 27(6), 595–602.

630 Chen, Y. and Or, D., 2006. Effects of Maxwell-Wagner polarization on soil complex dielectric
631 permittivity under variable temperature and electrical conductivity. Water Resources Research
632 42(6), W06424.

633 Colombano, S., Saada, A., Guerin, V., Bataillard, P., Bellenfant, G., Beranger, S., Hube, D.,
634 Blanc, C., Zornig, C. and Girardeau, I., 2010. Quelles techniques pour quels traitements–
635 analyse coûts-bénéfices. Rapport final BRGM-RP-58609-FR.

636 Colombano, S., Davarzani, H., Van Hullebusch, E. D., Ignatiadis, I., Huguenot, D., Guyonnet,
637 D. and Deparis, J., 2017. Drainage-imbibition tests and pumping of heavy chlorinated solvents
638 in saturated porous media: measurements and modeling of the effects of thermal and chemical
639 enhancement. 14th International AquaConSoil Conference-Sustainable Use and Management
640 of Soil, Sediment and Water Resources.

641 Coster, H., 1948. The electrical conductivity of rocks at high temperatures. Geophysical Journal
642 International 5, 193–199.

643 Dakhnov, V. N., 1962. Geophysical well logging: The application of geophysical methods;
644 electrical well logging. Colorado School of Mines.

645 Glover, P.W.J., 2015. Geophysical properties of the near surface Earth: Electrical properties. In
646 Treatise on Geophysics, Schubert, G. (Editor-in-chief). Elsevier: Oxford, Vol. 11, 89-137.

647 Grellier, S., Robain, H., Bellier, G. and Skhiri, N., 2006. Influence of temperature on the
648 electrical conductivity of leachate from municipal solid waste. Journal of Hazardous Materials
649 137(1), 612–617.

650 Grimm, R. E. and Olhoeft, G. R., 2004. Cross-hole complex resistivity survey for PCE at the
651 SRS A-014 outfall. Symposium on the Application of Geophysics to Engineering and
652 Environmental Problems, pp. 455–464.

653 Hayashi, M., 2004. Temperature-electrical conductivity relation of water for environmental
654 monitoring and geophysical data inversion. Environmental monitoring and assessment 96(1-
655 3), 119–128.

Hayley, K., Bentley, L., Gharibi, M. and Nightingale, M., 2007. Low temperature dependence of electrical resistivity: Implications for near surface geophysical monitoring. Geophysical Research Letters 34(18), L18402.

Heimovaara, T., Focke, A., Bouten, W. and Verstraten, J., 1995. Assessing temporal variations in soil water composition with time domain reflectometry. Soil Science Society of America Journal 59(3), 689–698.

Hwang, Y. K., Endres, A. L., Piggott, S. D. and Parker, B. L., 2008. Long-term ground penetrating radar monitoring of a small volume DNAPL release in a natural groundwater flow field. Journal of Contaminant Hydrology 97(1-2), 1–12.

Iordache, D., Niculae, D. and Hathazi, F. I., 2010. Utilization of microwave energy for decontamination of oil polluted soils. Journal of Microwave Power and Electromagnetic Energy 44(4), 213–221.

Kalmykov, Y. P., Coffey, W. T., Crothers, D. S. and Titov, S. V., 2004. Microscopic models for dielectric relaxation in disordered systems. Physical Review E 70(4), 041103.

Keller, G. V. and Frischknecht, F. C., 1966. Electrical methods in geophysical prospecting. Pergamon Press, Oxford.

Kizito, F., Campbell, C.S., Campbell, G.S., Cobos, D.R., Teare, B.L., Carter, B. and Hopmans, J.W., 2008. Frequency, electrical conductivity and temperature analysis of a low-cost capacitance soil moisture sensor. Journal of Hydrology, 352(3-4), 367-378.

Lakrari, K., El Moudane, M., Hassanain, I., Ellouzi, I., Kitane, S. and El Belghiti, M. A., 2013. Study of electrical properties of vegetable oils for the purpose of an application in electrical engineering. African Journal of Food Science 7(11), 404–407.

678 Lide, D.R. (Ed), 2008. Handbook of Chemistry and Physics, 89th Ed., CRC Press, Boca Raton,
679 NY, 6/154.

680 Llera, F. J., Sato, M., Nakatsuka, K. and Yokoyama, H., 1990. Temperature dependence of the
681 electrical resistivity of water-saturated rocks. Geophysics 55(5), 576–585.

682 Maineult, A., Bernabé, Y. and Ackerer, P., 2004. Electrical response of flow, diffusion, and
683 advection in a laboratory sand box. Vadose Zone Journal 3(4), 1180–1192.

684 Maineult, A., Revil, A., Camerlynck, C., Florsch, N. and Titov, K., 2017. Upscaling of spectral
685 induced polarization response using random tube networks. Geophysical Journal
686 International, 209(2), 948-960.

687 Malmberg, C. and Maryott, A., 1956. Dielectric constant of water from 0 to 100 °C. Journal of
688 Research of the National Bureau of Standards 56, 1–8.

689 Nath, J., 1995. Ultrasonic velocities, relative permittivities and refractive indices for binary
690 liquid mixtures of trichloroethene with pyridine and quinoline. Fluid Phase Equilibria
691 109(1), 39–51.

692 Nath, J. and Dubey, S., 1980. Binary systems of trichloroethylene with benzene, toluene, p-
693 xylene, carbon tetrachloride, and chloroform. ultrasonic velocities and adiabatic
694 compressibilities at 303.15 and 313.15 k, and dielectric properties and refractive indexes at
695 303.15 k. The Journal of Physical Chemistry 84(17), 2166–2170.

696 Nathanail, J., Bardos, P. and Nathanail, C.P., 2011. Contaminated land management: ready
697 reference. EPP Publications.

698 Noritomi, K., 1958. Migration of charged carrier in the case of electric conduction of rooks,
699 Science Reports of the Tohoku University, Ser. 5, Geophysics 9(3), 120–127.

700 Nouveau, M., Grandjean, G., Leroy, P., Philippe, M., Hedri, E. and Boukcim, H., 2016.
701 Electrical and thermal behavior of unsaturated soils: experimental results. Journal of Applied
702 Geophysics, 128, 115-122.

703 Pelton, W.H., Ward, S.H., Hallof, P.G., Sill, W.R. and Nelson, P.H., 1978. Mineral
704 discrimination and removal of inductive coupling with multifrequency IP. Geophysics, 43(3),
705 588-609.

706 Persson, M. and Berndtsson, R., 2002. Measuring nonaqueous phase liquid saturation in soil
707 using time domain reflectometry. Water Resources Research 38(5), 22–1-22-8.

708 Quist, A. S. and Marshall, W. L., 1968. Electrical conductances of aqueous sodium chloride
709 solutions from 0 to 800° and at pressures to 4000 bars. The Journal of Physical Chemistry
710 72(2), 684–703.

711 Raju, G.G. 2003. Dielectrics in electric fields. Dekker. 578p.

712 Richards, L.A., 1954. Diagnosis and Improvement of Saline and Alkali Soils. United States
713 Salinity Laboratory Staff. Agriculture Handbook No. 60, USDA and IBH Pub. Coy Ltd., New
714 Delhi, 98-99.

715 Riley, F., 1988, The Electronics Assembly Handbook, Springer, Berlin.

716 Romig, P., 2000. Seeing into the earth: Noninvasive characterization of the shallow subsurface
717 for environmental and engineering applications. National Academies Press.

718 Rosenbaum, U., Huisman, J., Vrba, J., Vereecken, H. and Bogena, H., 2011. Correction of
719 temperature and electrical conductivity effects on dielectric permittivity measurements with ech
720 2 o sensors. Vadose Zone Journal 10(2), 582–593.

721 Schweitzer, P. A., 2004. Corrosion resistance tables: metals, nonmetals, coatings, mortars,
722 plastics, elastomers and linings, and fabrics. CRC Press.

723 Scott, W. and Kay, A. E., 1988. Earth resistivities of Canadian soils, Canadian Electrical
724 Association.

725 Sen, P. N. and Goode, P. A., 1992. Influence of temperature on electrical conductivity on shaly
726 sands. Geophysics 57(1), 89–96.

727 Seyfried, M. S. and Grant, L. E., 2007. Temperature effects on soil dielectric properties
728 measured at 50 MHz. Vadose Zone Journal 6(4), 759–765.

729 Shah, Z. and Tahir, Q., 2011. Dielectric properties of vegetable oils. Journal of Scientific
730 Research 3(3), 481–492.

731 Sherrod, L., Sauck, W. and Werkema Jr, D. D., 2012. A low-cost, in situ resistivity and
732 temperature monitoring system. Groundwater Monitoring & Remediation 32(2), 31–39.

733 Snieder, R., Hubbard, S., Haney, M., Bawden, G., Hatchell, P., Revil, A. and DOE Geophysical
734 Moninitoring Working Group, 2007. Advanced noninvasive geophysical monitoring
735 techniques. Annual Review of Earth and Planetary Sciences 35, 653-683.

736 Sogade, J. A., Scira-Scappuzzo, F., Vichabian, Y., Shi, W., Rodi, W., Lesmes, D. P. and
737 Morgan, F. D., 2006. Induced-polarization detection and mapping of contaminant
738 plumesinduced-polarization mapping of contaminant plumes. Geophysics 71(3), B75–B84.

739 Stogryn, A., 1971. Equations for calculating the dielectric constant of saline water
740 (correspondence). IEEE Transactions on Microwave Theory and Techniques 19(8), 733–736.

741 Waxman, M. H. and Thomas, E., 1974. Electrical conductivities in shaly sands-i. the relation
742 between hydrocarbon saturation and resistivity index; ii. the temperature coefficient of
743 electrical conductivity. Journal of Petroleum Technology 26(02), 213–225.

744 Weast, R. C., 1986. Handbook of physics and chemistry. CRC Press, Boca Raton, 1983–1984.

745 Whitney, M. and Briggs, L. J., 1897. An electrical method of determining the temperature of
746 soils. USDA Division of Soils Bulletin 7, U.S. Government Printing Office, Washington, D.C.

747 Westerlaken, E., 1985. Rosin solder flux residues shape solvent cleaning
748 requirements. Electronic Packaging and Production, 25(2), 118-124.

749 Wightman, W., Jalinoos, F., Sirles, P. and Hanna, K., 2004. Application of geophysical
750 methods to highway related problems. Technical report No. FHWA-IF-04-021.

751 Zhu, H., Wang, W., Wang, H., Zhao, H. and Xin, M., 2018. Study on electrical properties of
752 coal at spontaneous combustion characteristic temperature. Journal of Applied Geophysics
753 159, 707–714.

754 **TABLES**

755 **Table 1** Physical characteristics of the DNAPL (CT and CS) used in experiments at 20°C

	Density (Kg/m^3)	**Viscosity (Pa.s)**	**Interfacial tension (mN/m)**	**Contact angle/glass (°)**
Coal tar (CT)	1099	0.054	2.5	128
Chlorinated solvent (CS)	1660	0.0045	11.15	60.67

756

757 **Table 2** Relative permittivity at 20°C (ε'_{20}) and coefficients of *a*, *b* and (R^2) (equation 5) for

758 different multiphase media used in this study

	ε'_{20}	*a*	*b*	R^2	*P-value*
GB+water	33.337	-0.0393	0.0001	0.9997	0.0117
GB+CT	11.476	0.0971	-5.00×10^{-5}	0.9996	0.0177
GB+CS	9.3644	0.0779	-0.0002	0.999831	0.0172

759

760

761

762 **FIGURES**

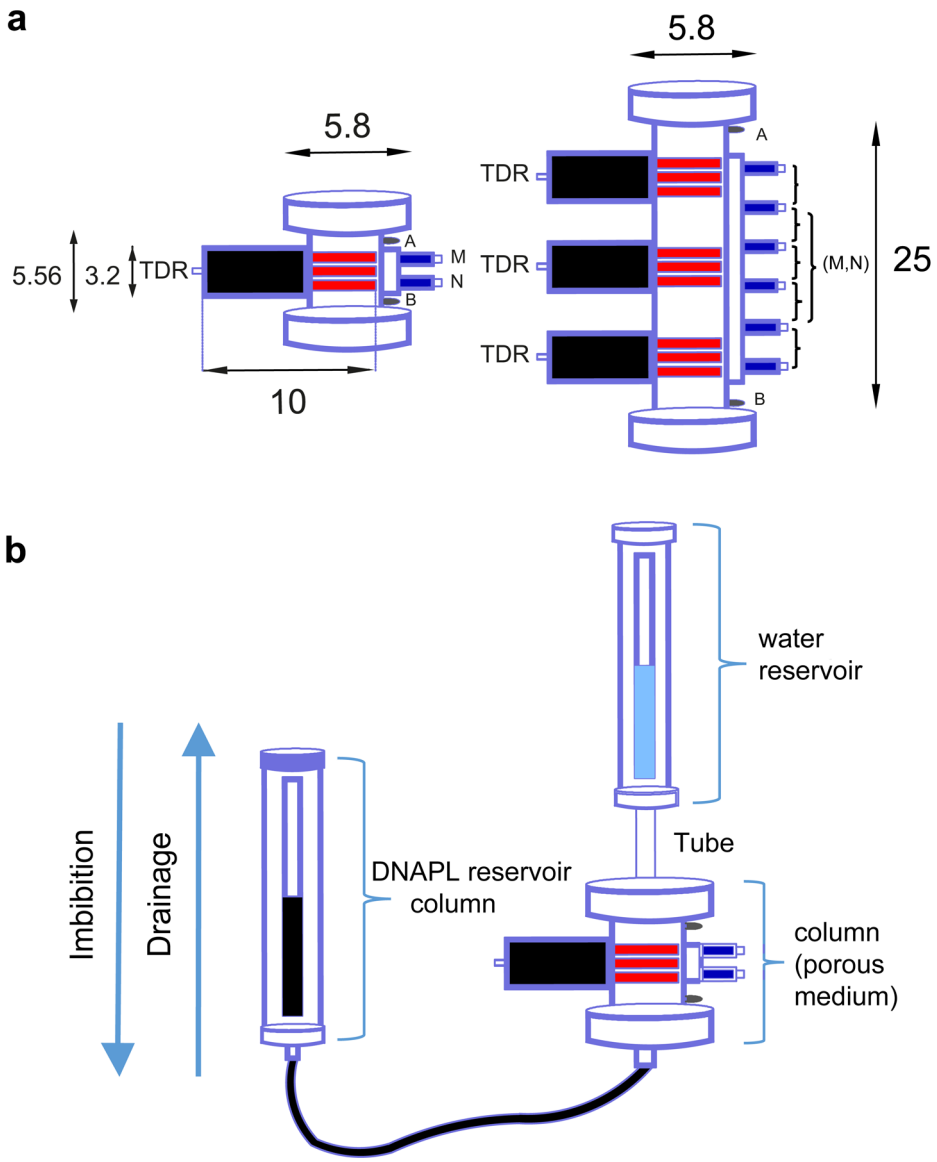

763

764 **Fig. 1.** Schematic of experimental setup (lengths are in cm). a) Geometry of a cell and a column
765 with the position of TDRs, current (A and B) and potential (M and N) electrodes. Each bracket
766 indicates a measurement in a sample. b) Experimental setup including water and DNAPL
767 reservoirs and sample.

768

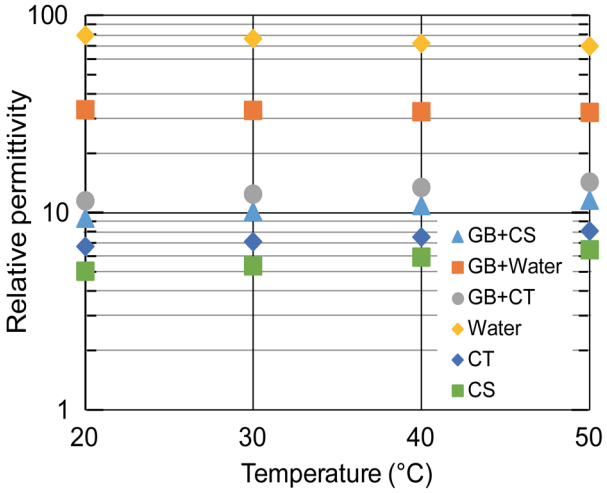

769

770 **Fig. 2.** Variations of relative permittivity as a function of temperature for pure products: CS,
771 CT, water, GB+CS, GB+CT and GB+water.

772

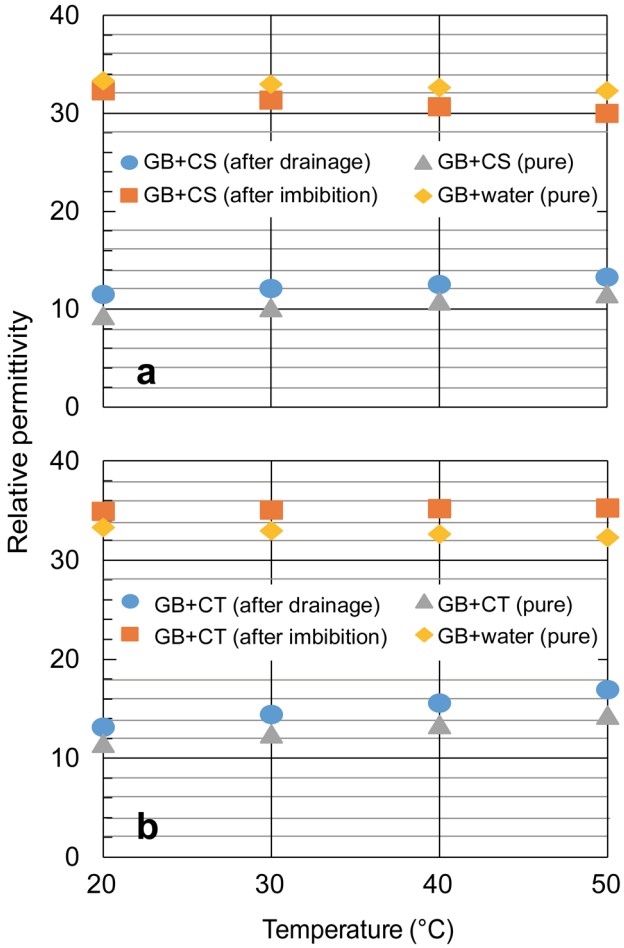

773

774 **Fig. 3.** Change in relative permittivity as a function of temperature for a) CS and b) CT after
775 drainage (80 % DNAPLs and 20 % water) and imbibition (92 % water and 8 % DNAPLs)
776 compared to the pure products.

777

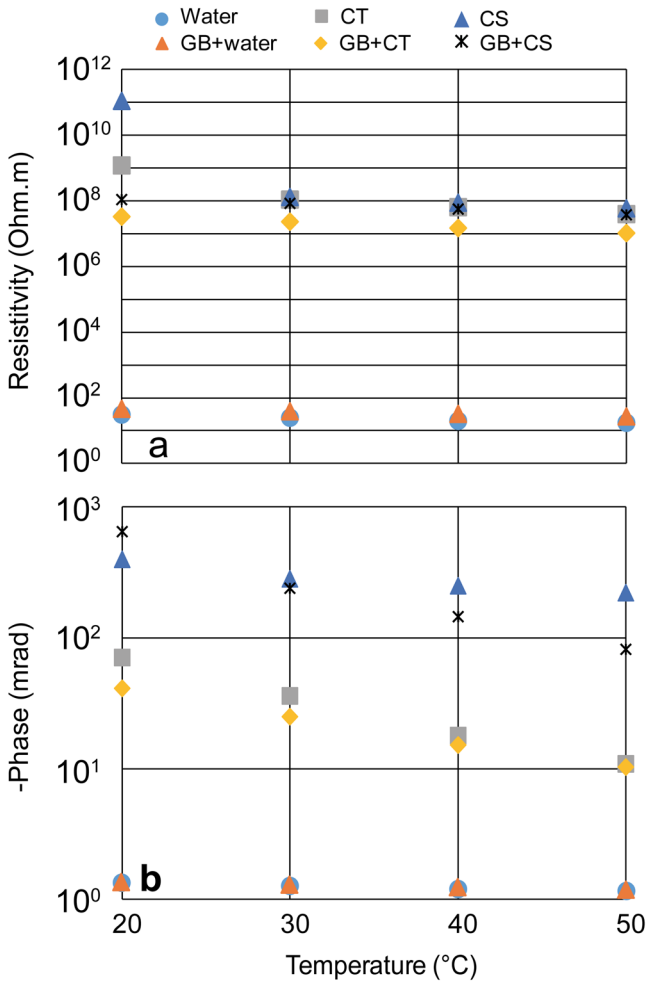

778

779 **Fig. 4.** Variation of (a) resistivity (real part of complex resistivity) and (b) phase (imaginary
780 part of complex resistivity) as a function of temperature at 1.46 Hz for pure products: CS, CT,
781 water, GB+CS, GB+CT and GB+water.

782

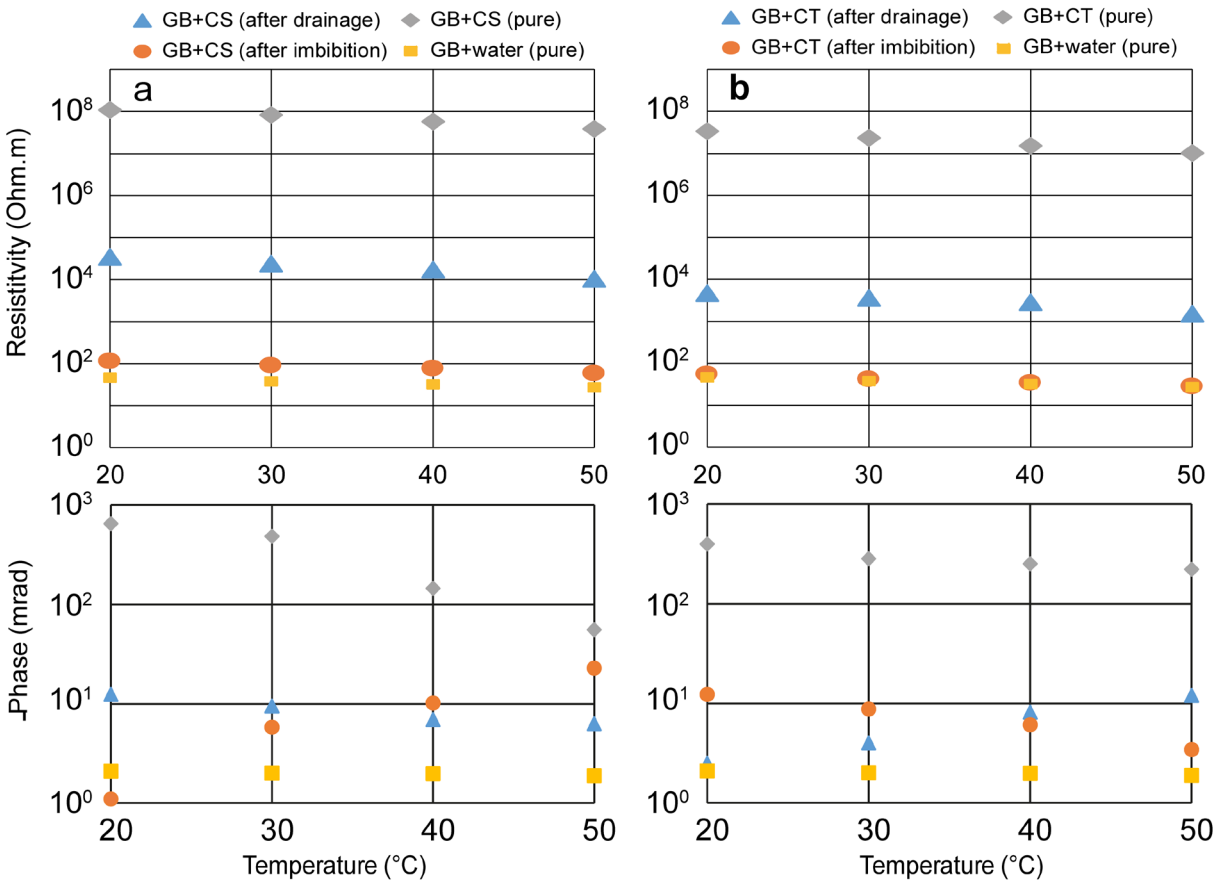

783

784 **Fig. 5.** Changes in electrical resistivity (a and b) and phase (c and d) as a function of
785 temperature at 1.46 Hz for CS and CT after drainage (80 % DNAPLs and 20 % water) and
786 imbibition (92 % water and 8 % DNAPLs) compared to the pure products.

787

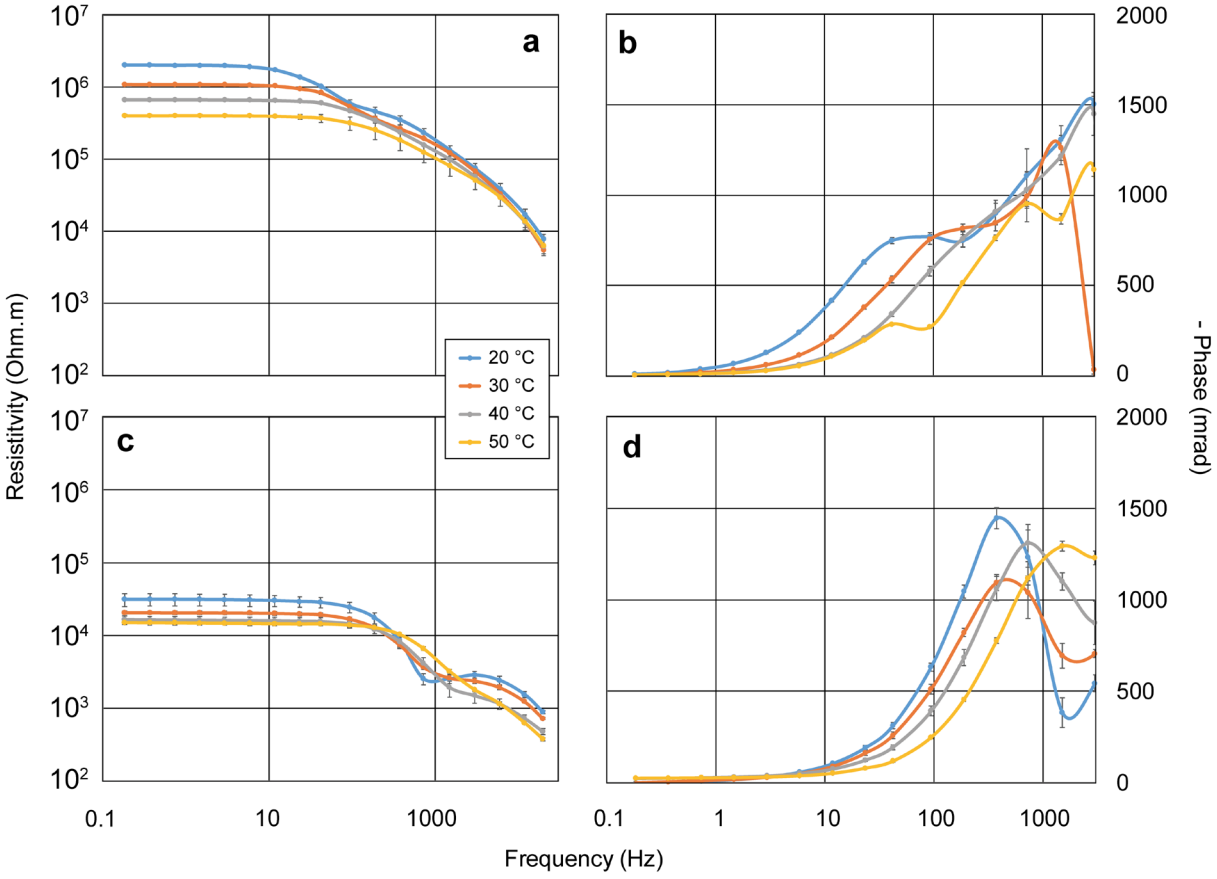

788

789 **Fig. 6.** SIP response and comparison between resistivity and phase spectra of samples with (a)
790 CT and (b) GB+CT as a function of temperature.

791

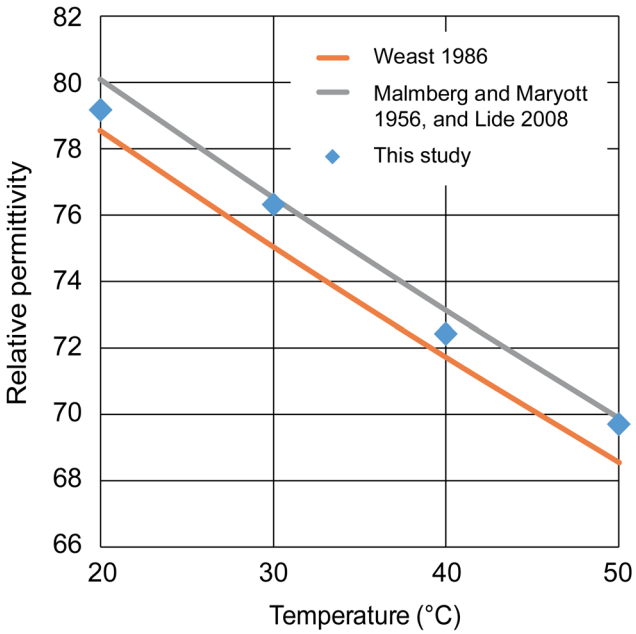

792

793 **Fig. 7.** Fitting of experimental data of relative permittivity with three empirical models (Lide,
794 2008; Weast, 1986; Malmberg and Maryott, 1956)

795

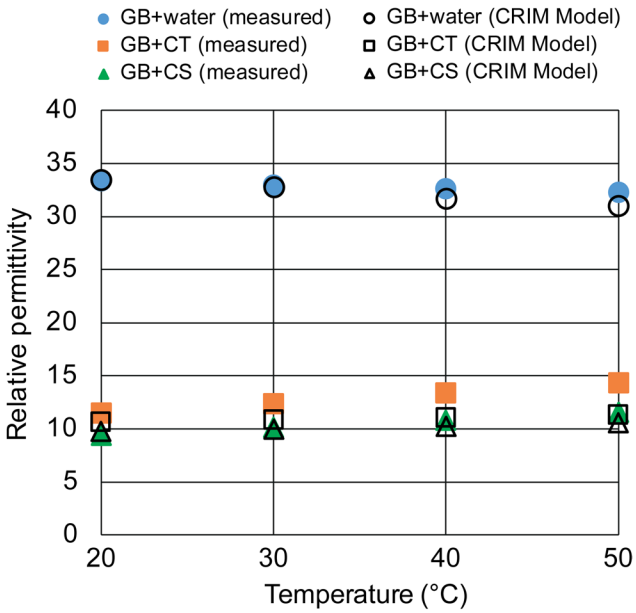

796

797 **Fig. 8.** Mixing model of experimental data of relative permittivity for different multiphase
798 systems

799

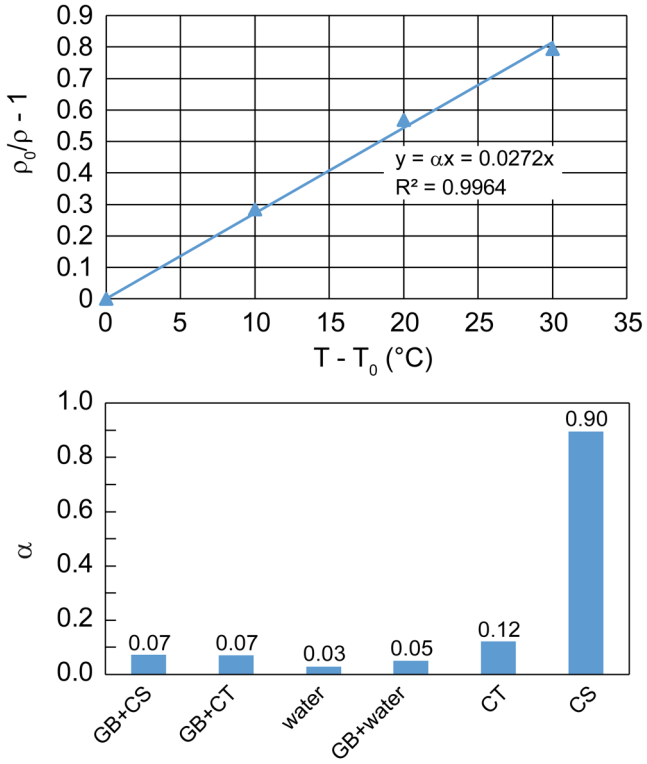

800

801 **Fig. 9.** (a) An example of using linear regression to obtain α value for water (b) comparison
802 between α values obtained for water, CT and CS, with and without GB (f=1.46 Hz).

803

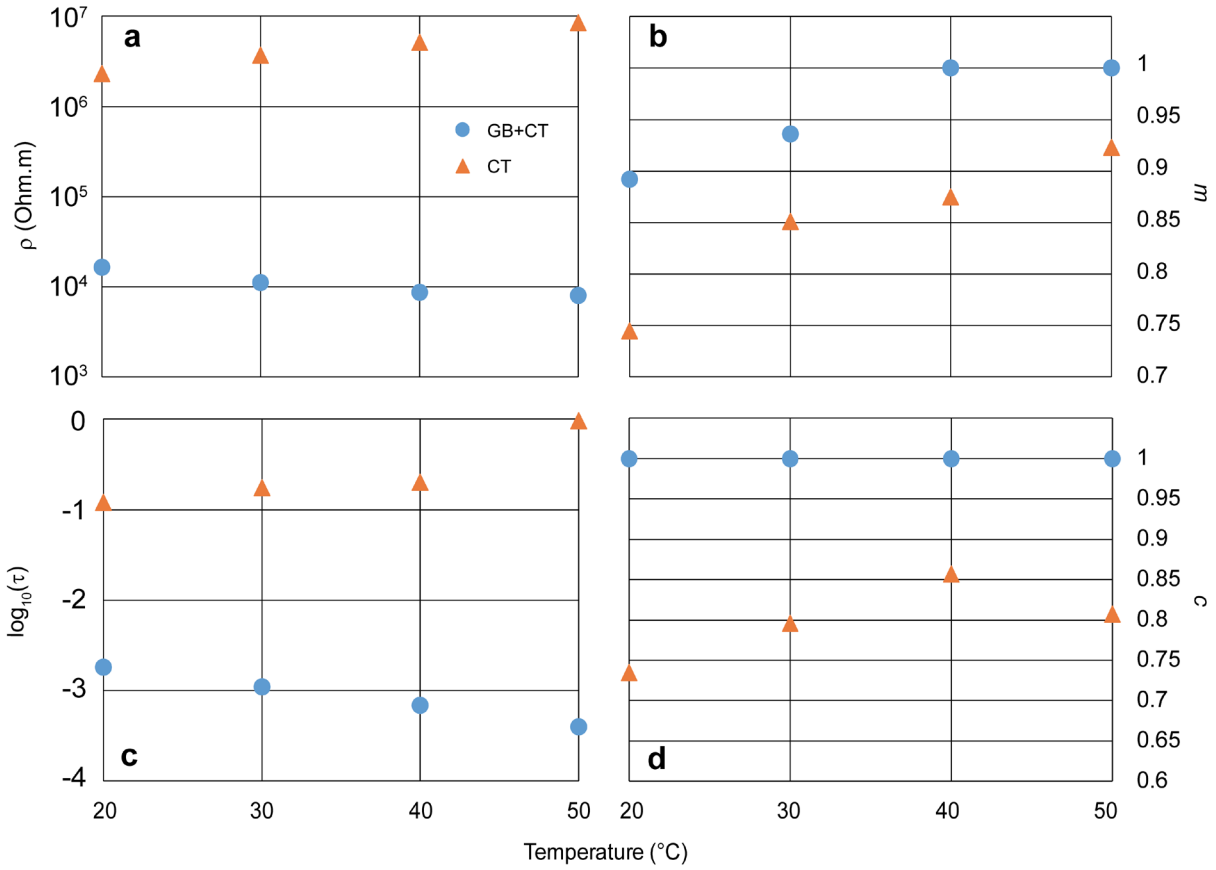

804

805 **Fig. 10.** Cole-Cole parameters as a function of temperature for CT, with and without GB.

806